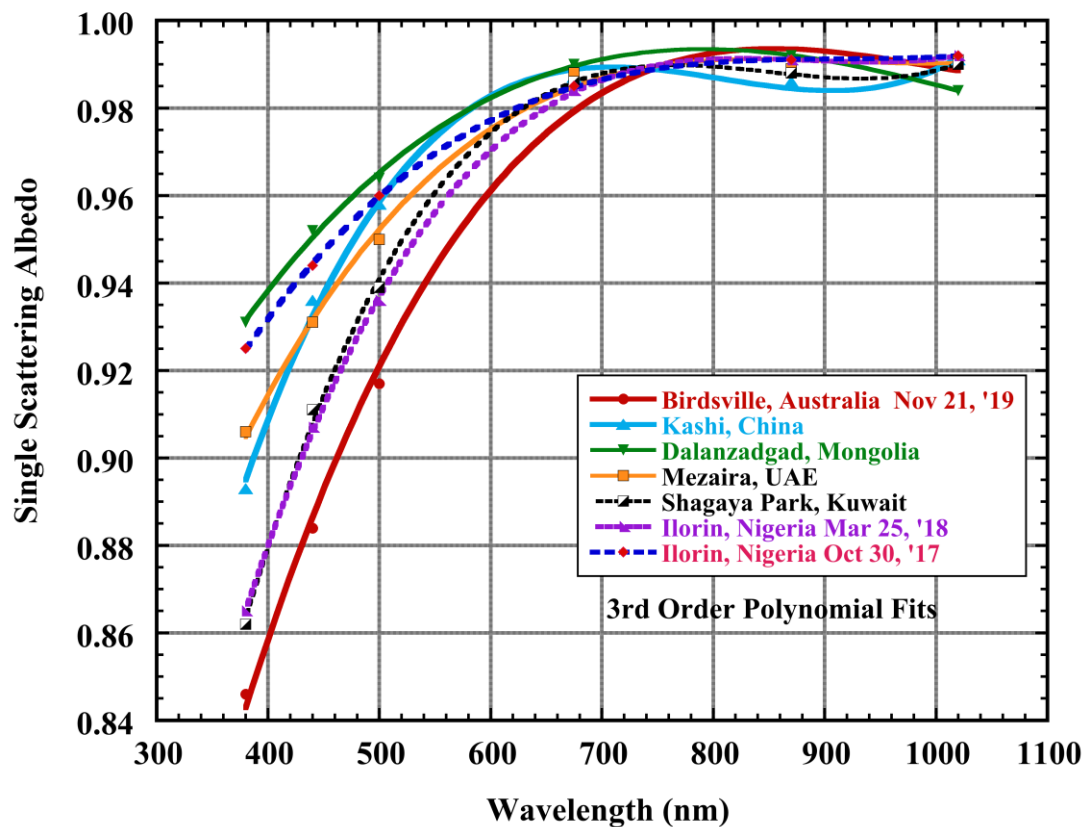


Analysis of AERONET Extended Wavelength Retrievals of Aerosol Absorption Parameters Including 380 nm and 500 nm for Detection of Brown Carbon in Biomass Burning and Iron Oxides in Desert Dust

Thomas F. Eck^{1,2}, Brent N. Holben², Alexander Sinyuk^{3,2}, David M. Giles^{3,2}, Ilya Slutsker^{3,2}, Joel S. Schafer^{3,2}, Mikhail G. Sorokin^{3,2}, Alexander Smirnov^{3,2}, Anthony D. LaRosa^{3,2}, Jason Kraft^{4,2}
 (1) Universities Space Research Association, Columbia, MD, USA; (2) NASA/GSFC, Greenbelt, MD, USA; (3) Science Systems Applications, Inc., Lanham, MD, USA; (4) Fibertek Inc., Herndon, VA, USA

Dust Events (AE<0.4) - AERONET Single Scattering Albedo
 T-Cimels Level 2 except Birdsville L1.5



Comparison of spectral SSA from AERONET retrievals (AE<0.4) from various dust sources and/or regions: Most weakly absorbing dust at 380 nm from Ilorin with trajectory from the Bodele, also a case from Mongolia. Strongest absorption from Australia (red soils with high iron oxides). Similar SSA at all sites for $\lambda > 600$ nm.

Comparison of AERONET retrievals to in situ Lab measurements

Atmospheric Chemistry and Physics | EGU

Complex refractive indices and single-scattering albedo of global dust aerosols in the shortwave spectrum and relationship to size and iron content

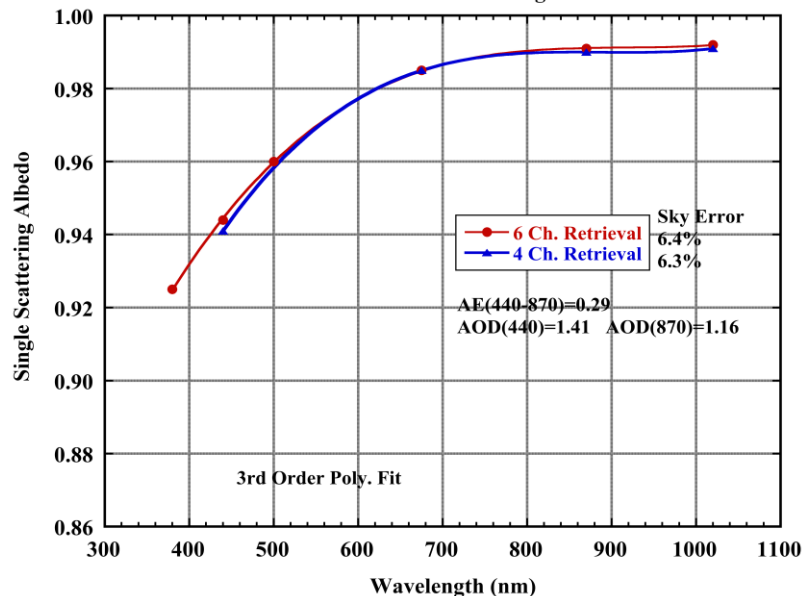
Claudia Di Biagio¹, Paula Formenti¹, Yves Balkasakis², Lorenzo Caporaso¹, Mathieu Canhaman¹, Edouard Pangai¹, Emille Jourdain¹, Sophie Nemecek¹, Mehrez G. Andreou³, Konrad Kanold⁴, Barbara Simeoni⁵, Stuart Platt⁶, David Sotgiu¹, Earle Williams¹, and Jean-François Doussin¹

Table 5. As in Table 4 for the single-scattering albedo (SSA) data. Mean, m

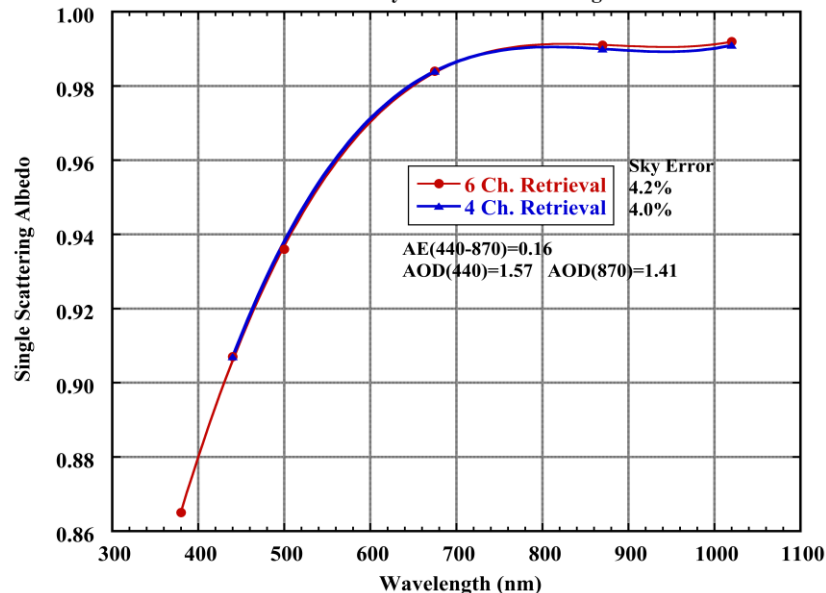
Sample region	SSA						
	0.37 μm	0.47 μm	0.52 μm	0.59 μm	0.66 μm	0.88 μm	0.95 μm
Tunisia	0.85	0.90	0.93	0.95	0.95	0.97	0.97
Morocco	0.92	0.95	0.96	0.98	0.98	0.98	0.99
Libya	0.89	0.93	0.95	0.98	0.98	0.98	0.98
Algeria	0.87	0.92	0.94	0.97	0.97	0.98	0.98
Mauritania	0.85	0.90	0.94	0.96	0.97	0.98	0.98
NAF-S	0.88	0.92	0.94	0.97	0.97	0.98	0.98
Niger	0.72	0.85	0.89	0.91	0.92	0.94	0.95
Mali	0.75	0.85	0.89	0.93	0.95	0.96	0.96
Bodélé	0.96	0.98	0.98	0.99	0.99	0.99	0.99
SAH	0.81	0.89	0.92	0.94	0.95	0.96	0.97
Ethiopia	0.80	0.86	0.90	0.92	0.94	0.97	0.97
Saudi Arabia	0.88	0.93	0.96	0.98	0.98	0.98	0.98
Kuwait	0.95	0.97	0.98	0.98	0.99	0.99	0.99
EAF-ME	0.88	0.92	0.94	0.96	0.97	0.98	0.98
Gobi	0.88	0.92	0.94	0.96	0.97	0.97	0.97
Taklimakan	0.82	0.88	0.92	0.95	0.96	0.96	0.96
EA	0.85	0.90	0.93	0.96	0.96	0.97	0.97
Arizona	0.93	0.96	0.97	0.98	0.98	0.99	0.99
NAM	0.93	0.96	0.97	0.98	0.98	0.99	0.99
Atacama	0.89	0.93	0.94	0.97	0.97	0.98	0.98
Patagonia	0.88	0.91	0.94	0.96	0.97	0.98	0.98
SAM	0.89	0.92	0.94	0.96	0.97	0.98	0.98
Namib-1	0.91	0.95	0.96	0.98	0.98	0.99	0.99
Namib-2	0.74	0.82	0.86	0.92	0.94	0.96	0.97
SAF	0.83	0.88	0.91	0.95	0.96	0.98	0.98
Australia	0.70	0.81	0.85	0.91	0.93	0.96	0.97
AUS	0.70	0.81	0.85	0.91	0.93	0.96	0.97
Mean	0.85	0.91	0.93	0.96	0.96	0.97	0.98
Median	0.88	0.92	0.94	0.96	0.97	0.98	0.98
10 %	0.74	0.84	0.88	0.92	0.94	0.96	0.96
90 %	0.93	0.96	0.97	0.98	0.99	0.99	0.99

Di Biagio et al. (2019) measured spectral absorption in a laboratory from soil samples collected from around the world. Soil dust was suspended in a smog chamber for measurements of scattering and absorption coeff. to be made. The least absorbing dust came from samples taken in the Bodele, with SSA at 370 nm of 0.70. From the AERONET cases shown in the plot at left the most absorbing is from Birdsville, Australia with SSA at 380 nm ~0.84, while the least absorbing is from Mongolia and Ilorin, Nigeria ~0.93. For the weakly absorbing case in Nigeria the back trajectory suggests some origin from over the Bodele Depression. Therefore we see general agreement in the dust source regions for strongly and weakly absorbing particles, although the extremes are much greater in the lab data of Di Biagio et al. (2019). This may be due in part to dust from several sources mixing together in the transported aerosol plumes measured by AERONET.

Ilorin, Nigeria - Dust Case Oct 30, 2017
Level 2 SZA=58.4 deg.



Ilorin, Nigeria - Dust Case Mar 25, 2018
Level 2 Hybrid SZA=45.87 deg.

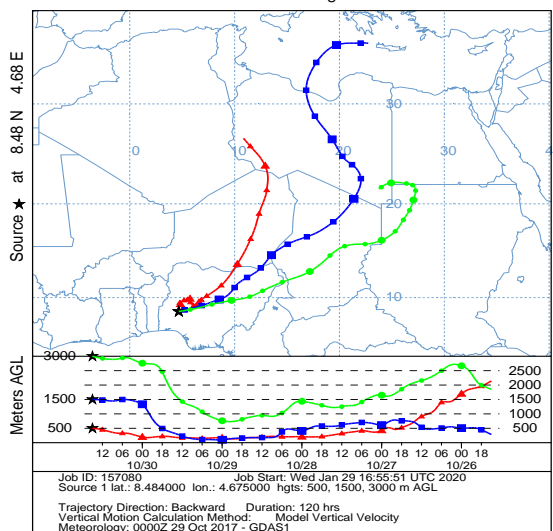


Ilorin, Nigeria AERONET site

Significant differences in dust absorption on different dates of large dust events ($AOD(440) > 1.4$ for both).

Back trajectories suggest that dust in these events originated from different source regions

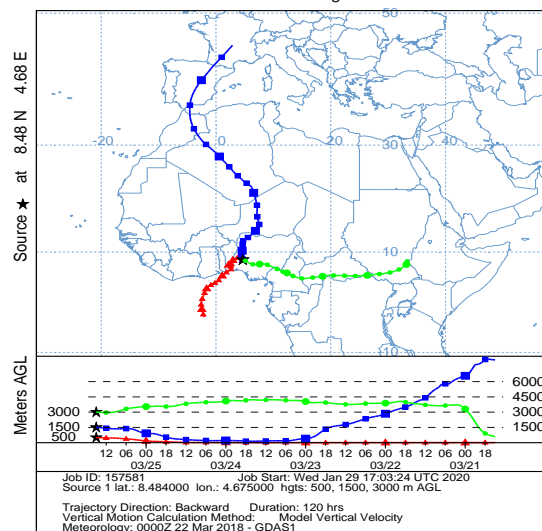
NOAA HYSPLIT MODEL
Backward trajectories ending at 1500 UTC 30 Oct 17
GDAS Meteorological Data



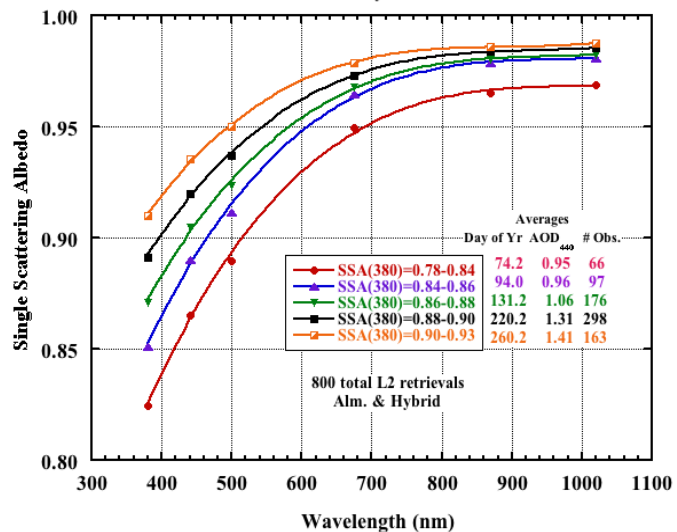
Oct. 30, 2017 trajectory in blue passes directly over the Bodele Depression which is a source of very weakly absorbing diatomite sediments.
Mar 25, 2018 trajectory in blue passes over a different region of the Sahara, not even close to the Bodele Depression.

The higher SSA in the Oct 30, 2017 retrievals is consistent with the characteristics of the mineral source in the Bodele Depression

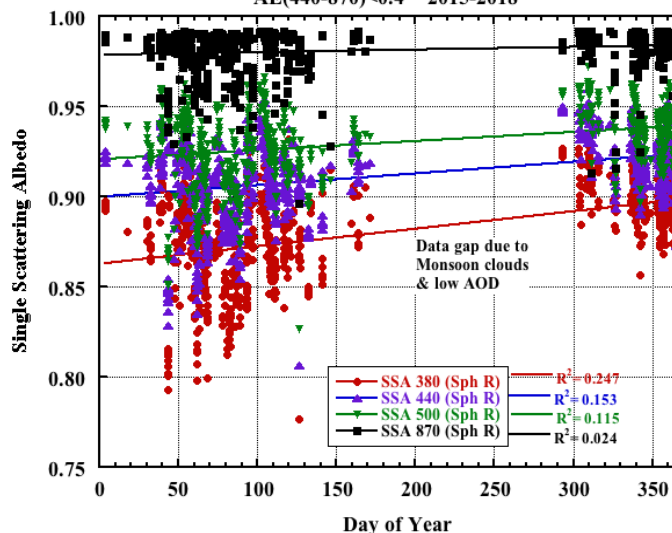
NOAA HYSPLIT MODEL
Backward trajectories ending at 1500 UTC 25 Mar 18
GDAS Meteorological Data



ILORIN, Nigeria Dust Cases Sphere Cal, Relax AE(440-870)<0.4
2015-2018 Sorted by SSA at 380 nm



ILORIN, Nigeria Dust Cases Sphere Cal, Relax
AE(440-870)<0.4 2015-2018

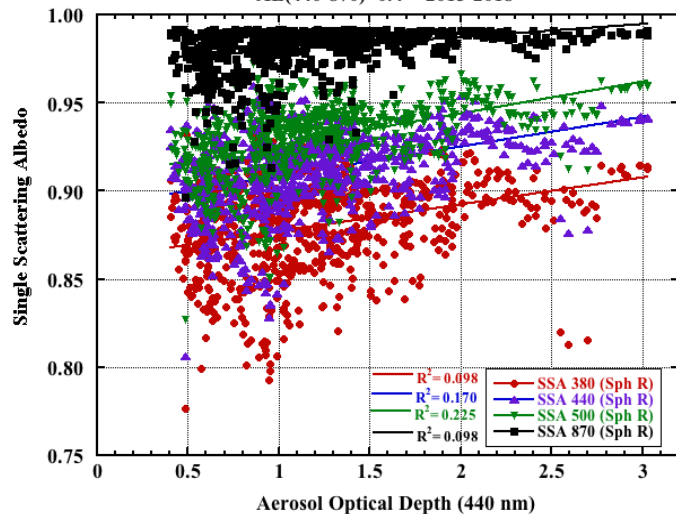


Ilorin, Nigeria:

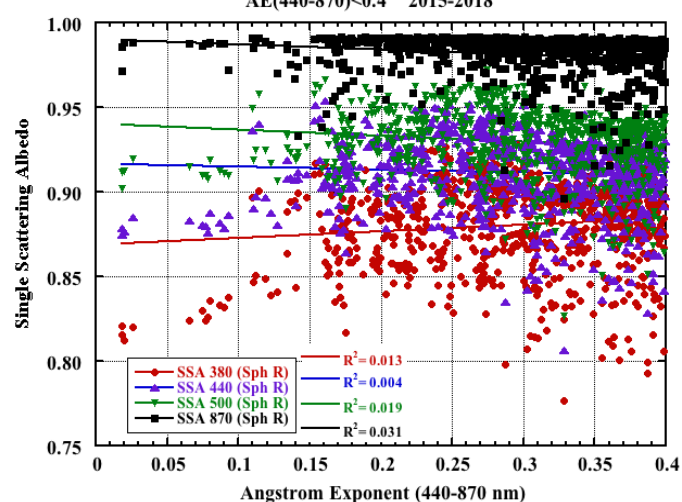
SSA from Feb-May is lower at shorter wavelengths than from October - December, possibly due to more transport from the Bodele to Ilorin in the fall season.

SSA increases as AOD increases, possibly in part due to the Bodele Depression events having both very high AOD and very low SSA (weak absorption in diatomaceous sediment versus iron oxides in mineral dust)

ILORIN, Nigeria Dust Cases Sphere Cal, Relax
AE(440-870)<0.4 2015-2018

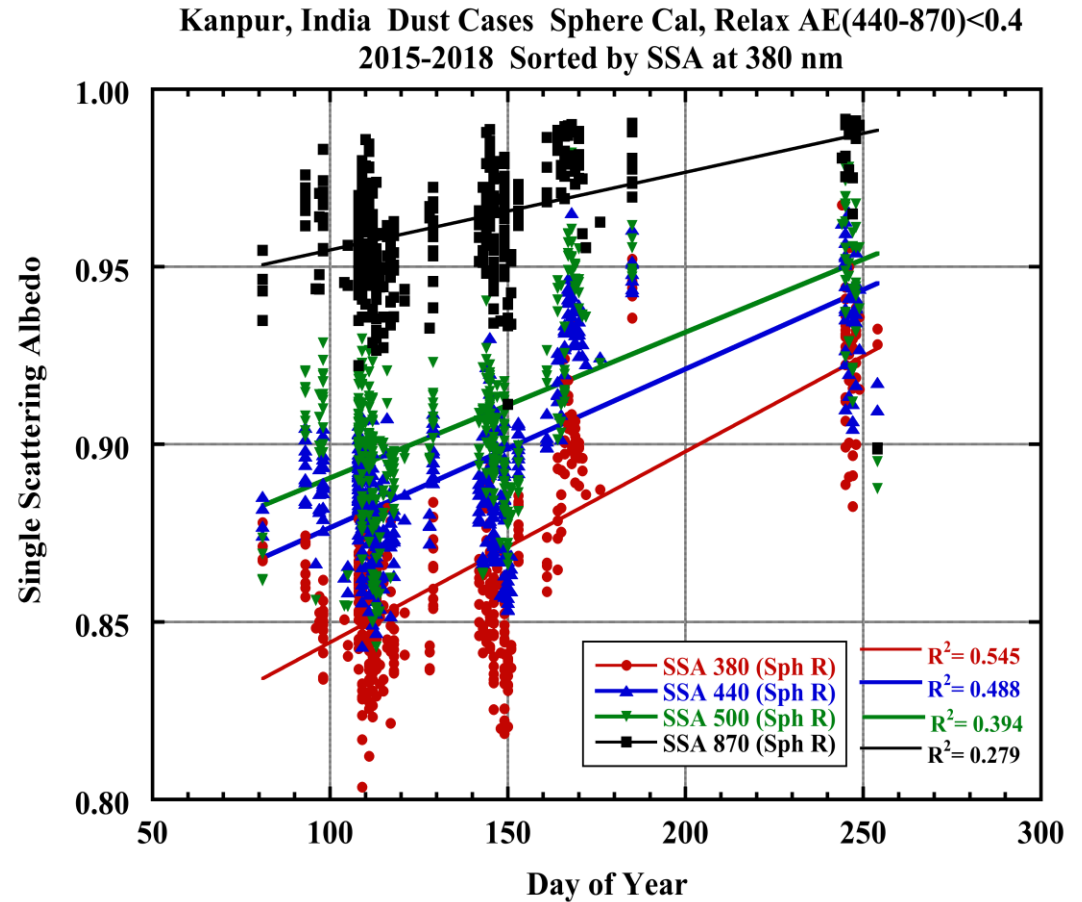
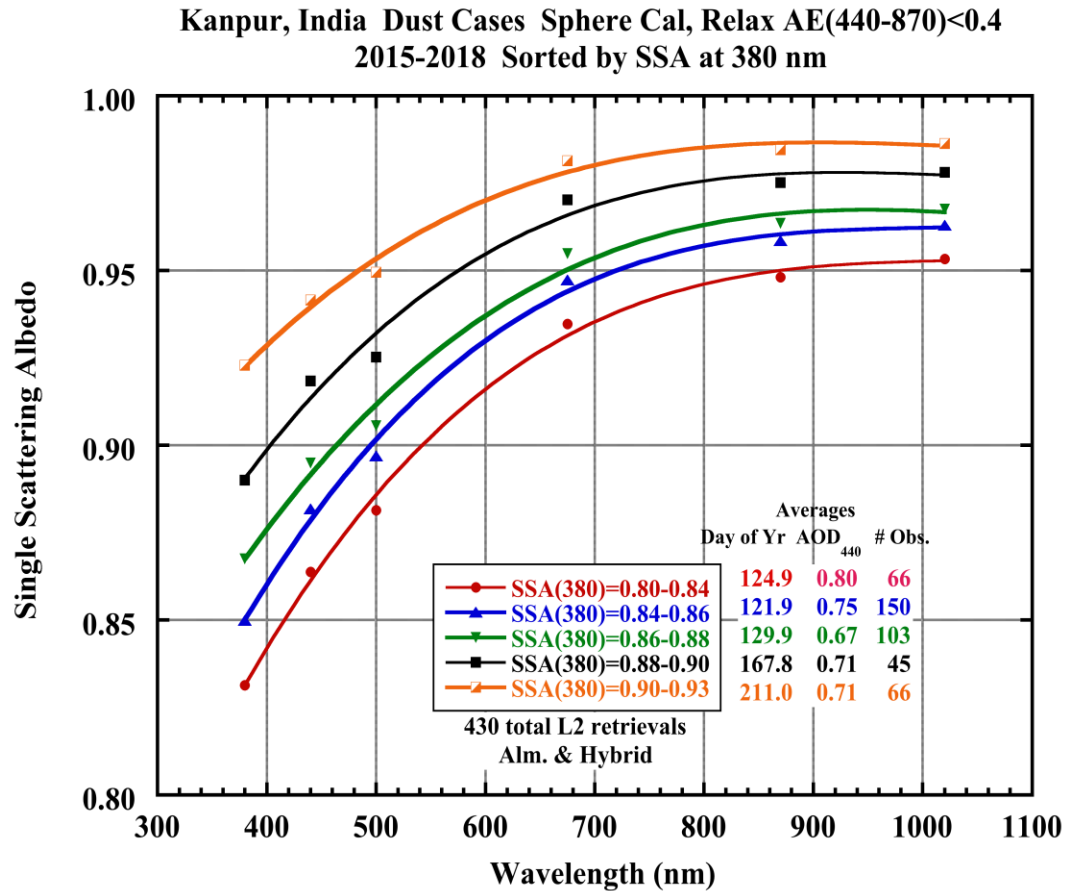


ILORIN, Nigeria Dust Cases Sphere Cal, Relax
AE(440-870)<0.4 2015-2018



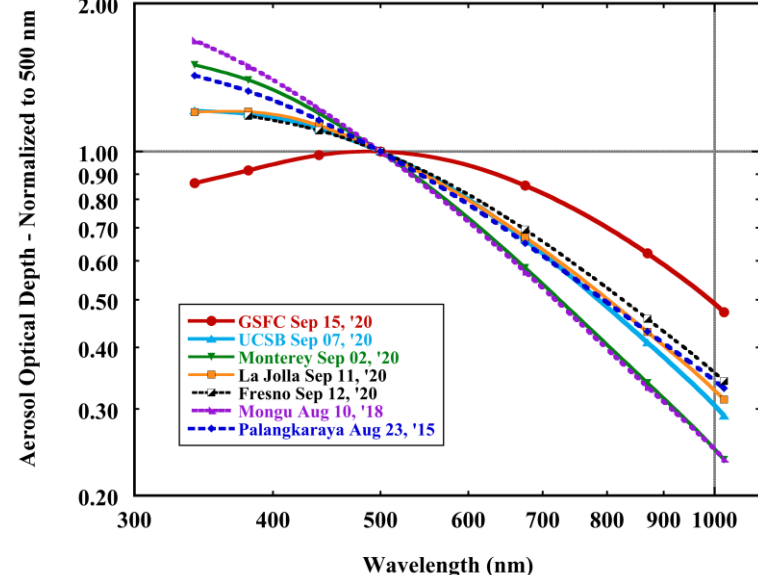
The data gap in January is likely due to lack of AE<0.4 due to biomass burning smoke mixing with dust

Kanpur, India: Strong trend of decreasing absorption through the spring to fall seasons at all wavelengths, greatest at shortest wavelengths (possible BC coating on dust - note that longer λ SSA increases also); no trend as a function of AOD; trend as a function of AE is only significant at longer wavelengths ($r^2=0.25$ at 870 nm)

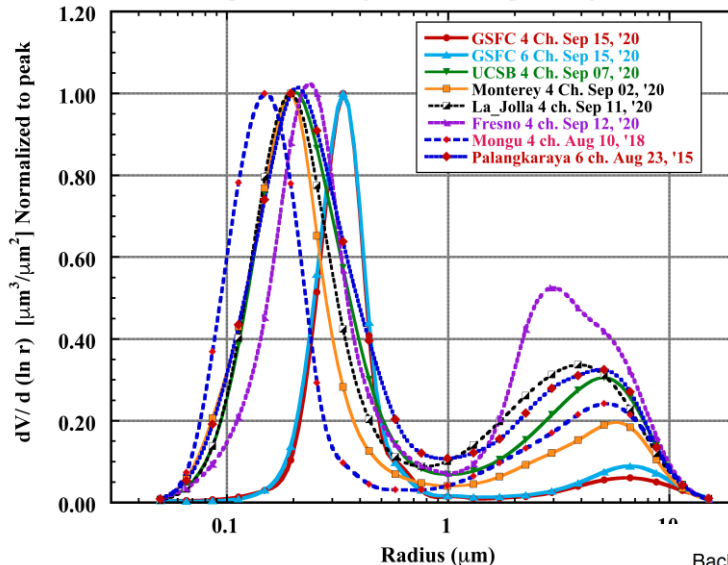


GSFC Sep 15, '20: Long distance smoke transport from California

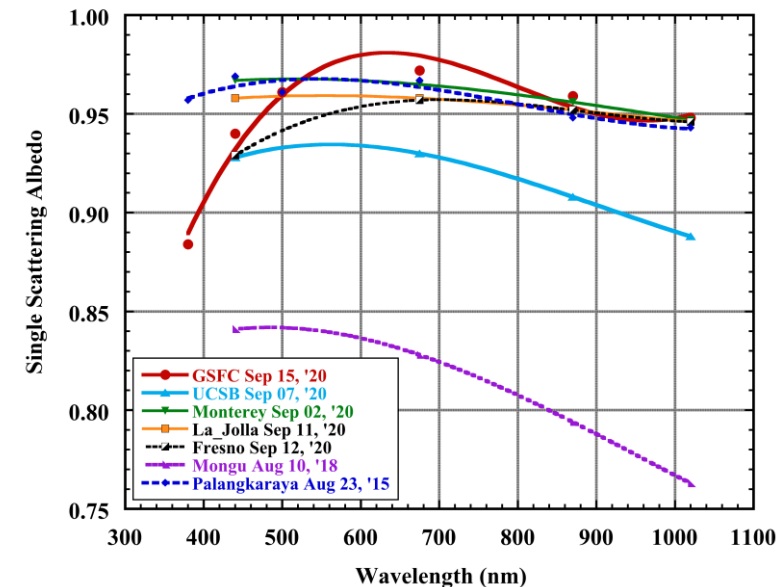
Biomass Burning Smoke Size Distribution Comparisons
GSFC Sep 15, '20 - Long Distance transported aged smoke



Biomass Burning Smoke Size Distribution Comparisons
GSFC Sep 15, '20 - Long Distance transported aged smoke

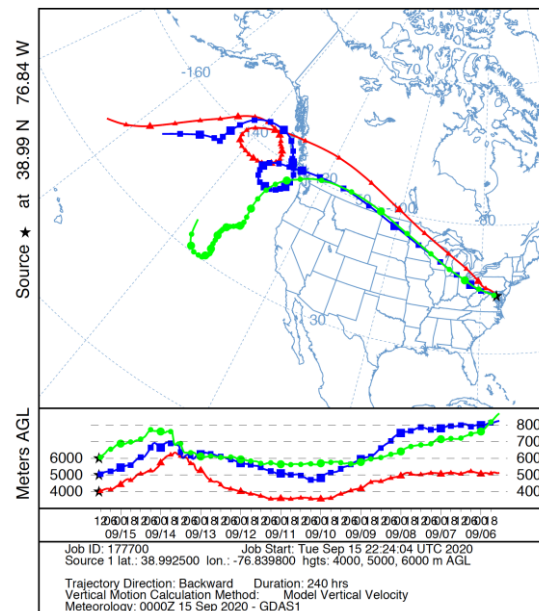


Biomass Burning Smoke Size Distribution Comparisons
GSFC Sep 15, '20 - Long Distance transported aged smoke



- **Normalized (to 500nm) AOD spectra at GSFC show extremely unusual decreases <500 nm.** At the La Jolla, UCSB and Fresno cases the AOD spectra show at flattening from 380 to 340 nm, when this smoke was close to the fire sources.
- **Normalized size distributions (to peak concentration values) comparisons to the GSFC case on Sep 15, '20 shows fine mode is significantly larger in radius and also much narrower in width**
- **Spectral SSA at GSFC for the Sep 15, '20 case shows strong absorption at 380 nm relative to 500 nm suggesting significant Brown Carbon absorption,** but also due to decreased scattering optical depth <500 nm due to the large size with narrow width fine mode size distribution
- AOD computed from the retrieved size distribution and refractive indices for the GSFC case matches the measured AOD to within 0.001 at all channels.

NOAA HYSPLIT MODEL
Backward trajectories ending at 1300 UTC 15 Sep 20
GDAS Meteorological Data



HYSPLIT Back-Trajectory shows that the air that arrived at GSFC at 6 km on Sep 15 was located over the Pacific off the west coast of California and Oregon from Sep 8 through Sep 12, 2020. MPL backscatter at GSFC showed aerosol layer at 4-6 km altitude on Sep 15. This smoke is aging for a few days in an elevated layer over the Pacific Ocean, with some input from active fires each day, until it is advected towards the East coast (Sep 10 Aqua image below)

